Nov 24th

Load Tests on Steel-stud Walls

J. F. McDermott

Load Tests on Steel-Stud Walls

by

J. F. McDermott

Summary

Information required for steel-stud wall design was provided by a series of axial-compression tests and lateral-load tests conducted on solid-web and slit-web steel studs in wall panels with different sheathing materials and also on single studs.

* Associate Research Consultant, U. S. Steel Research Laboratory, Monroeville, Pa.

Introduction

The AISI "Specification for the Design of Cold-Formed Steel Structural Members"1)* applies to the design of solid-web steel studs with or without full lateral (in the plane of the wall) support, but does not apply directly to the design of (1) thermal (slit-web) studs regardless of support conditions or (2) solid-web studs with unsymmetrical partial support, that is, with exterior sheathing attached to one face of the studs but no interior sheathing attached to the other face.

To obtain design information necessary for such use of wall studs, three types of tests were performed: (1) wall-compression tests of three-stud specimens with sheathing on either one or both sides, (2) lateral-loading (bending) tests of five-stud specimens with sheathing on either one or both sides, and (3) axial-compression tests of single-stud specimens without any intermediate lateral support, that is, without any support except at the ends of the stud. For each type of test, both solid and slit-web channel-shaped cold-formed galvanized steel studs with stiffening lips were tested to provide a direct comparison of strengths.

---

* See References.

Materials and Experimental Work

Studs

As shown in Figure 1, the Super-C solid-web steel stud has 1-1/2-inch (38.1 mm) flanges, 1/2-inch (12.7 mm) stiffening lips, and either a 3- or a 3-1/2-inch-deep (76.2 or 88.9 mm) web. Hereafter, this solid-web steel stud will be referred to as the "solid" stud. The Super-C thermal slit-web stud, shown in Figure 2, has the same basic dimensions as the solid stud, but its web has a special pattern of longitudinal slits that reduce the conductance of heat across the web. Hereafter, this stud will be referred to as the "slit" stud. Typically, the top and bottom of the studs rest inside the transverse steel runner shown in Figure 1. Both the solid and the slit studs were produced from ASTM A446 Grade C galvanized steel. The testing was limited to 3-1/2-inch deep 20-gage and 18-gage solid and slit studs because it was anticipated that problems which could cause premature failures (that is, twisting, buckling) would be more critical in these specimens than in other commercially available studs of these types.

Wall-Compression Tests

Details of the wall panels used in the wall-compression tests are given in Table I. Generally, each specimen was constructed with a 90- by 72-inch (2.29 by 1.83 m) frame, Figure 3, consisting of three 90- or 89.5-inch-long (2.29 or 2.27 m) 18- or 20-gage steel studs on 24-inch (0.61 m) centers. Load-distribution assemblies, shown in Figure 4, were connected to both the top and bottom of each specimen before testing. Sheating was attached to either one or both sides of the frame. The type of sheathing and the screw spacing along the studs are listed in Table I.

Each wall-compression test specimen was placed vertically in the testing frame as shown in Figure 3. Details of the support at the top and bottom of the specimen appear in cross section in Figure 4. Load was applied by a 50-kip-capacity (222 kN) hydraulic jack reacting downward on a top spreader beam as shown in Figure 3. The load was transferred from the top spreader beam through two curved bearing bars to a beam which rested continuously on the specimen load distribution assembly.

Lateral-Load Tests

Details of the wall panels used in the lateral-loading tests are given in Table II. Generally, each specimen was constructed with a 90- by 97-5/8-inch (2.29 by 2.48 m) frame, Figure 5, consisting of five 87-inch-long (2.21 m) 18- or 20-gage studs, 24 inches (0.61 m) on center. Sheathing was attached to either one or both sides of the frame. The type of sheathing and the screw spacing along the studs are listed in Table II.

A plastic air bag, placed between the specimen and a reaction system, was inflated during the test to apply a uniform load. The top and bottom edges of the specimen reacted against beam assemblies that were held down by rods connected to load cells. Contact between the specimen and each beam assembly was a 1-1/2-inch-diameter steel bar located on the center steel plate positioned over the 2 by 4 wood sill or header of the test specimen. The test setup simulated uniform wind loading on a wall spanning 86 inches (2.18 m) between simple-beam end supports. For specimens with sheathing on only one side, the unsupported flange was in tension, as it would be in applications where the sheathing has been applied to the exterior face only.

Single-Stud Compression Tests

Details of the single-stud compression tests are given in Table III. The specimens were 96- or 20-inch-long (2.44 m or 0.51 m) 18-gage slit and solid studs.

The 20-inch-long studs were tested in a universal testing machine with bearing surfaces fixed against rotation; thus, the effective column length was 10 inches (25.4 cm). The test arrangements for the 96-inch-long studs are shown in Figure 6. A 1/4-inch-thick (6.35 mm) steel plate was welded to each end of each stud, and the specimen was then placed in a vertical position, about 2-1/2 inches (6.35 cm) away from a vertical wide-flange column that was connected to a test frame. Each end plate of the stud was bearing against a 1/4-inch-thick plate having a 1-inch-diameter (25.4 mm) half pin welded to the outer horizontal surface and opposite the stud. Thus, the effective length of each stud was

98 inches (2.49 m) measured between the outer surfaces of the top and bottom half pins. Each outer plate was adjusted, with the help of four horizontal set screws, so that the centerline of each half pin coincided with the weak axis of bending of the stud. The top half pin was bearing against a top bracket that was bolted to the wide-flange column. The bottom half pin was bearing against a plate welded to a guided piston that was free to twist. The specimen was loaded by a 20-kip-capacity (89 kN) jack that was inserted between the piston and a bottom bracket that was bolted to the wide-flange column. The center of the half pin at the stud end was aligned with the centerline of the piston.

Test Results

Wall-Compression Tests

Deflections. A typical load-deflection curve for a wall-compression test is given in Figure 7. The average axial deflection over a 78-inch (1.98 m) height is shown. The experimental vertical deflections were slightly less than the theoretical axial deflections based only on axial shortening (the dashed line) for a solid stud without sheathing. The difference was probably due either (1) to slip between the stud and the sheathing, so that the axial deflection of the sheathing was less than that of the stud, or (2) to composite action of the sheathing with the stud, resulting in a decrease in the axial deflection. The difference was somewhat smaller for Tests 3, 4, 12, and 13 where sheathing was on only one side. The theoretical axial shortening due to the observed lateral (perpendicular to the wall) deflections never exceeded 0.003 inch (0.08 mm).

Progressively increasing lateral bending (perpendicular to the sheathing) occurred in all tests, probably because the studs were not exactly straight and because the axial loads did not consistently pass through the centroids of the stud cross sections, despite the precautions taken to achieve purely axial loading by the use of the round bearing bars centered with respect to the studs, Figure 4.

The initial out-of-straightness, y_o, that would cause a given lateral deflection, Δ, is approximately equal to

$$y_o = \frac{\Delta \left(1 - \frac{P}{P_e}\right)}{\frac{P}{P_e}} \tag{1}$$

The eccentricity, e, of loading (distance from the axial load to the axis of bending at each end of the stud) that would cause a given lateral deflection, Δ, is approximately equal to

$$e = \frac{8EI_{xx}\Delta}{PL^2}\left[1 - \frac{P}{P_e}\right] \tag{2}$$

In these equations, P is the test axial load, P_e is the Euler load determined as 1.92[2)] times the gross area times F'_e as defined on page 23 of Reference 1, E is the modulus of elasticity (29,500 ksi or 203 GN/m^2), I_{xx} is the strong-axis moment of inertia, and L is the length of the stud measured center-to-center of the assumed pinned ends. Since both y_o and e are constants by definition, either Equation 1 or 2 implies that Δ varies in proportion to

$$\frac{P}{1 - \frac{P}{P_e}}$$

Then, each P - Δ plot, such as in Figure 7, would be a smooth convex-upward curve, with the ratio of Δ at half the maximum load to Δ at the maximum load ranging from 0.34 for Test No. 2, to 0.41 for Test No. 12. Because the P - Δ plots for lateral deflection did not generally follow this pattern exactly, values of y_o or e calculated for any test vary according to the values of P used in calculating them.

For the 13 tests, the values of y_o corresponding to maximum load ranged from 0.090 to 0.418 inch (2.13 to 10.6 mm) and averaged 0.264 inch (6.7 mm). The values of e ranged from 0.072 to 0.339 inch (1.8 to 8.6 mm) and averaged 0.214 inch (5.4 mm). Thus, either a small initial out-of-straightness or a small eccentricity would cause the observed lateral deflection at maximum load. Furthermore, a combination of even smaller values of y_o and e would cause these lateral deflections.

Mode of Failure. All wall-compression tests terminated by a sudden unloading, with little or no apparent yielding before failure. In the specimens with sheathing on one side only, the unsupported stud flange moved parallel to the wall as the result of twisting of the cross section at failure. At failure, local buckles usually occurred in the flange near midheight in two or three of the studs in the specimen, as illustrated in Figure 8. Since tests and theoretical calculations showed that local buckling occurs in the flange only after yielding, it is probable that these local flange buckles did not initiate failure, but rather occurred after failure was initiated by column or lateral-flexural buckling.

Both wall-compression-test specimens with 20-gage solid studs formed local buckles at the bottoms of the studs. Those local buckles can be attributed to the fact that the flanges of these particular studs had been chamfered to fit into a narrow track. It appears that the local buckles at the bottoms of the studs did not limit the loading sustained by the specimen with no interior sheathing (Test No. 13) because it developed a flange buckle at a location more than 2 feet (0.6 m) above the base. However, the local buckles at the base apparently did limit the load capacity of the specimen with sheathing on both sides

(Test No. 10) since no other cause of the unloading was apparent. Therefore, Test No. 10 was considered invalid.

Maximum Loads. The maximum loads of the wall-compression tests are listed in Table I and compared with calculated ultimate loads based on the AISI specification.[1)] Specifically, the ultimate load for the specimen was calculated by multiplying the allowable strong-axis column-buckling load (AISI Section 3.6.1.1)[1)] for a single solid stud by the AISI factor of safety of 1.92[2)] and by 3 to account for the number of studs in the specimens. Two sets of comparisons giving ratios of experimental data to corresponding theoretical data are made. In the first comparison, the theoretical force is based on the measured thicknesses and yield points of the tested studs. In the second comparison, the theoretical force is based on the nominal thicknesses (for the given gages) and the 40-ksi (276 MN/m^2) specified minimum yield point of A446, Grade C galvanized steel. In both sets of comparisons, the sheathing is neglected except as it provides lateral support.

In addition to ultimate loads based on axial load alone, ultimate loads based on bending in combination with axial load were calculated and are listed in Table I. The bending moment used in these calculations was equal to the maximum experimental axial load times the apparent eccentricity computed as explained above in the section on Deflections. With bending present, the axial-load capacity is reduced by the factor[1,2)]

$$\left[1 - \frac{f_b}{(1 - \frac{P}{P_e})F_y}\right]$$

where f_b is the bending stress and F_y is the yield point. Consequently, this factor was used to calculate theoretical ultimate axial loads that included the effect of unintentional eccentricities in the tests. In determining the factor, f_a and f_b were computed from the maximum test load, and F_y was the actual yield point of the steel.

In comparison with the theoretical loads based on the nominal thicknesses and the specified yield point, the behavior of the wall-compression specimens with sheathing attached on both sides can be summarized as follows:

Type of Stud	Range of Ratios Test Load ÷ Theoretical Load
Slit	0.84 to 1.13
Solid	1.10 to 1.17*

In comparison with the theoretical loads based on the measured thicknesses and yield points, the performance of the specimens with sheathing attached on both sides can be summarized as follows:

* Excluding invalid Test No. 10

Type of Stud	Range of Ratios: Test Load ÷ Theoretical Load	Range of Ratios: Ratio Including Bending
Slit	0.72 to 0.99	0.90 minimum
Solid	0.89 to 0.97	1.25 minimum*

The solid studs, which conform to the AISI specification,[1)] should attain ratios (not including bending) exceeding 0.87 (that is, 1.0 ÷ 1.15), since the AISI allowable stresses in axial compression incorporate a safety factor (1.92) about 15 percent larger than the basic safety factor of 1.67 used in most parts of the specification to account "for the greater sensitivity of compression members to accidental imperfections of shape or accidental load eccentricities, when compared to tension members or beams."[2)] This ratio (0.87) was exceeded in all valid solid-steel tests. As expected, the ratios for the slit studs did not always exceed 0.87.

For the two sets of tests on solid and slit studs with sheathing on one side only (Tests 3 and 4, and 12 and 13), the ratios of test to theoretical load (computed by using either actual or nominal thicknesses and yield points) ranged from 0.60 to 0.87, and were well below the ratios for studs with sheathing on both sides.

Using actual thicknesses and yield points, comparisons between slit and solid studs were obtained by dividing the ratio (not including bending) for a slit stud by the ratio for a similar

* Excluding invalid Test No. 10.

(same gage and same sheathing) solid stud. The results ranged from 0.77 to 0.97.

Lateral-Loading Tests

Deflections. A typical load-deflection curve is given in Figure 9 for a lateral-loading test. For the solid studs with sheathing on both sides, the experimental curves were close to and slightly to the right of the theoretical curves (neglecting sheathing), indicating that the sheathings did not contribute significantly to the bending stiffness of the panels. For all the other lateral-loading tests, the experimental deflections were somewhat greater than theoretically predicted for solid studs (neglecting the sheathings). For the specimens with sheathing on only one side, this may be attributed to twisting of the studs during the test, Figure 10, which causes a decrease in the effective depths of the studs. For the slit-stud specimens with sheathing on both sides, the greater deflections can be attributed to a decrease in stiffness caused by the slits.

Modes of Failure. In most tests, failure was gradual, with the central portions of the studs tending to rotate, as indicated in Figure 10. This can be attributed to the combined effect of (1) twisting which occurs because the lateral loading is not being applied to the stud through the shear center, and (2) the tendency for the loaded sheathing to deform grossly, causing the attached flange of the stud to rotate about the stud web, which acts as a fulcrum. These effects are more pronounced if the strength or stiffness of the loaded (exterior) sheathing is less or if there is no interior sheathing. The specimens generally unloaded immediately after the formation of a crack in the interior gypsum-board sheathing at the location of a stud, or when fiberboard exterior sheathing cracked or the stud "knifed through" the fiberboard.

Maximum Loads. The maximum lateral loads are listed in Table II and are compared with the lateral loading that theoretically would cause the start of yielding of solid studs. As in Table I, two sets of comparisons with the experimental data are made: (1) with the theoretical force based on measured thicknesses and yield points and (2) with the theoretical force based on the nominal thicknesses and the 40-ksi (276 MN/m^2) specified minimum yield point of A446, Grade C galvanized steel. In both sets of comparisons, the sheathing is neglected, except as it provides in-plane support.

In comparison with the theoretical loadings based on the nominal thicknesses and the specified yield point, the behavior of the specimens with sheathing attached on both sides can be summarized as follows:

Type of Stud	Range of Ratios Test Load ÷ Theoretical Load
Slit	0.95 to 1.35
Solid	1.21 to 1.47

In comparison with the theoretical loadings based on the measured thicknesses and yield points, the performance of the specimens with sheathing attached on both sides can be summarized as follows:

Type of Stud	Range of Ratios Test Load ÷ Theoretical Load
Slit	0.78 to 1.30
Solid	0.86 to 1.57

The high ratios, 1.30 and 1.57, correspond to specimens in which Panel 15 sheathing was connected to the studs by screws at a spacing considerably less than that used for the other specimens with Panel 15 sheathing. The solid studs, which conform to the AISI specification,[1)] would be expected to attain ratios of about 1. The only solid-stud ratio less than 1 (0.86 for the 20-gage stud, Test No. 26), corresponded to a steel with a 53-ksi (365 MN/m^2) yield point, which is considerably greater than the 40-ksi minimum yield point specified for the studs. This lower ratio is probably explained by the rupture of the exterior sheathing that occurred when the net upward pressure was only 79.7 psf (3816 N/m^2), which was 13.3 psf (637 N/m^2) less than the ultimate load. Apparently, the premature rupture of the exterior sheathing resulted from forces caused by the tendency of the studs to twist. Subsequently, the attached compression flanges of the studs were not sufficiently restrained against bending parallel to the wall. This caused premature failure of the studs at a loading corresponding to a computed stress of about 46 ksi (317 MN/m^2) rather than to the 53-ksi yield point.

As expected, the ratios of test to theoretical load for the slit studs did not always exceed 1. The load ratios for solid and slit studs with sheathing on one side only were generally well below 1. Using actual thicknesses and yield points, comparisons between slit and solid studs were obtained by dividing the ratio for a slit stud by the ratio for a similar (same gage and same sheathing) solid stud. The results ranged from 0.83 to 1.15.

Single-Stud Compression Tests

Modes of Failure. All the 96-inch-long single-stud specimens unloaded after bowing in the direction of weak-axis bending. Therefore, the failures of these specimens would be generally classified as weak-axis column buckling. In a few specimens, a slight twist was noticeable, suggesting some torsional-flexural buckling interacting with the weak-axis buckling. However, there was no consistent correlation between incidence of twisting and type of stud.

The 20-inch-long (0.51 m) single-stud specimens unloaded after forming local buckles. The local buckles of the solid studs occurred suddenly and were confined to short lengths, Figure 11, but the local buckles of the slit studs occurred gradually and extended over most of the specimen lengths, Figure 12.

Maximum Loads. The maximum axial loads for the single-stud specimens are listed in Table III and compared with calculated ultimate loads based on the AISI specifications.[1] Specifically, the ultimate load was the least load calculated by multiplying either the weak-axis column-buckling load (AISI Section 3.6.1.1)[1] or the torsional-flexural buckling load (AISI Section 3.6.1.2)[1] for a solid stud by the AISI factor of safety of 1.92.[2] These loads were nearly the same. For example, for the 96-inch-long stud the theoretical weak-axis column buckling load, based on an effective length of 98 inches, was 3.54 kips (15.7 kN) for the slit studs and 3.31 kips (14.7 kN) for the solid studs, whereas the corresponding torsional-flexural buckling loads were 3.28 kips (14.6 kN) and 3.10 kips (13.8 kN). For the 96-inch-long studs, the weak-axis column buckling load was the Euler buckling load, P_e.

Comparisons are made on the basis of both measured and nominal thicknesses and yield points. There was not much difference between the two sets of comparisons. The only ultimate loads on the 96-inch-long studs that were less than the theoretical allowable loads specified by AISI were those of one slit stud, with a ratio of test to theoretical maximum load of 0.96. The ultimate loads on the three long slit studs were less than the Euler buckling load, with a ratio of test to Euler buckling load ranging from 0.89 to 0.99. As expected, the ultimate loads on all the three long solid studs exceeded the Euler buckling load.

The ultimate loads on the 20-inch-long studs, with 10-inch (0.25 m) effective lengths, were generally less than the theoretical loads. The least ratio of the test load to the theoretical load based on measured thicknesses and yield points was 0.77 for slit studs and 0.91 for solid studs.

Design Method for Slit Studs

In the wall-compression tests of slit-stud specimens with sheathing on both sides, the ratio of test load to theoretical solid-stud load (based on measured thicknesses and yield points) exceeded 0.80 if the effect of the unintentional eccentricity was included in the theoretical load, and was never less than 0.72 if the effect of the eccentricity was not included. In the double-sheathing lateral-loading tests with slit studs, the ratio of test load to theoretical solid-stud load ranged from 0.78 to 1.30. In all the compression tests of the 96-inch-long single slit studs, the ratio of test load to theoretical load exceeded 0.80, and the ratio of test load to Euler buckling load, P_e, was 0.89 or greater.

Thus, the test results indicate that the design of slit studs for axial load, strong-axis bending, or a combination of both can safely be based on allowable stresses equal to 80 percent of the AISI allowable stresses for a solid stud of the same dimensions and steel, with the Euler buckling stress, F_e', also multiplied by 80 percent in the AISI interacting equations. This approach, of course, does not apply to studs supported by sheathing on one flange only since the AISI allowable stresses do not apply to this case, which is discussed later.

Lateral Support

Double Sheathing. The results of both the wall-compression and lateral-loading tests on specimens with sheathing on both sides of solid or slit studs suggest that the type of sheathing and spacing of connectors has some effect on ultimate strength. For example, the ultimate bending strength of specimens with Panel 15 attached to the exterior face by closely spaced screws was significantly greater than the ultimate strength of specimens with wider spacings or screws or with other sheathing materials. However, there are not enough data to define quantitatively the effect of various combinations of type of sheathing and type and spacing of connectors.

In both the wall-compression and lateral-loading tests, all the solid-stud specimens reached their theoretical ultimate loads except the specimen in lateral-loading test No. 26. As discussed previously, failure of this specimen was attributed to premature failure of the exterior fiberboard sheathing after attainment of the specified yield point of 40 ksi (276 MN/m^2) but before attainment of the actual yield point of 53 ksi (365 MN/m^2). Thus, all the tested combinations of sheathing and connector spacing provided full lateral support for solid-stud walls if the yield strength of the stud material does exceed about 45 ksi (310 MN/m^2).

In both the wall-compression and lateral-loading tests, many of the slit-stud specimens failed at loads significantly below the theoretical ultimate loads. Although most of the reduction probably resulted from the web slits, it is possible that sheathing failures may have contributed to the reduction in some tests, as discussed earlier. If there are any such effects, however, they are included in the multiplication factor of 80 percent for slit studs that was suggested previously. Consequently, if the multiplication factor is applied, all tested combinations of type of sheathing and connector spacing can be considered to provide full lateral support for slit-stud walls.

Single Sheathing Without Horizontal Strapping or Bracing. The ratios of the load sustained by a specimen with sheathing on only one side to the load sustained by a similar specimen with sheathing on both sides ranged from 0.71 to 0.87 for wall-compression tests and from 0.55 to 0.91 for lateral-loading tests. The lowest ratios, 0.71 and 0.55, were for the solid-stud comparisons; the lowest ratios for the slit-stud comparisons were 0.80 for the wall-compression tests and 0.67 for the lateral-loading tests. The loads for specimens with sheathing on one side only ranged from about 2.3 to 2.7 times the theoretical loads for studs with no lateral support. The loads for the specimens with sheathing on one side only were probably affected by the type of sheathing but there were not enough data to define the effect quantitatively.

Therefore, it is recommended that the design allowable stresses for either slit or solid studs with full lateral support be multiplied by a factor to obtain the corresponding design allowable stresses for studs with sheathing on only one side. On the basis of the available test results, it is suggested that the factor be 0.70 for allowable axial stress and 0.50 for allowable bending stress when the bending stress is tension in the unsupported flange. If the bending stress is compression in the unsupported flange, the allowable bending stress can be conservatively determined by assuming a stud with no lateral support. Since these multiplication factors probably depend considerably on the dimensions (unsupported length, etc.) of the specimens, they should not be used in applications where the dimensions are considerably different from those in the tests.

<u>Single Sheathing With Horizontal Strapping or Bracing</u>. As discussed in Reference 3, the effect of supports by horizontal strapping or bracing is to reduce the unsupported length of a stud in the weak-axis direction to the vertical distance between these supports or the distance between a support and the top or bottom of the stud. Therefore, where sheathing is attached to one side of the studs and horizontal strapping or bracing (but no sheathing) is attached to the other side, the allowable stresses may be determined by either of two methods: (1) calculation based on a stud with sheathing attached to one side and no lateral support on the other

side or (2) calculation based on a stud unsupported between straps or a strap and an end of the stud. The larger of these two allowable loads can be safely used in designing studs for either axial compression, bending, or a combination of both.

Conclusions

The results of the tests showed that walls with slit Super-C studs can be designed by using an allowable axial-compression or bending stress in the slit studs that is 0.80 times the AISI[1)] allowable stress for a similar solid stud. Designs governed by combined bending and axial compression may be computed for the slit Super-C stud by using these reduced allowable stresses and also the Euler buckling stress, F'_e, likewise multiplied by 0.80, in the AISI interaction equations.

All the tested sheathing materials (fiberboard, gypsum board, plywood, and Panel 15) and connection methods provide full lateral support for solid or slit Super-C studs loaded in axial compression or bending if the sheathing is attached to both flanges. If the sheathing is attached to only one flange (the compression flange for bending), the axial-compression strength is reduced by 30 percent and the bending strength by 50 percent compared with the corresponding strengths for a stud with full lateral support. In bending applications, if the sheathing is attached only to the tension flange, the stud should be designed as if it has no lateral supports.

References

1. "Specification for the Design of Cold-Formed Steel Structural Members, Cold-Formed Steel Design Manual—Part I," 1968 Edition, American Iron and Steel Institute, New York.

2. "Commentary on the 1968 Edition of the Specification for the Design of Cold-Formed Steel Structural Members," American Iron and Steel Institute, New York, 1970.

Table I

Wall-Compression Tests

Gage	Test No.	Sheathing* Exterior Side	Sheathing* Interior Side	Spacing of Screw Fasteners, inches Exterior Side	Spacing of Screw Fasteners, inches Interior Side	Type of Stud	Type of Track+	Uncoated Thickness of Stud, inch	L= Height of Specimen C-C Pins, inches	L/Rxx = Slenderness Ratio for Strong-Axis Buckling	Fy= Yield Point of Stud Steel, ksi	Q = AISI Area Factor	Ptest= Maximum Total Load on Specimen, kips	Theoretical Load++ Based On Measured Thickness and Yield Point: Ptheo, kips	Ptest/Ptheo	Ratio Including Bending	Theoretical Load++ Based On Nominal Thickness+++ and Yield Point: Ptheo, kips	Ptest/Ptheo
18	1	LG Fiberbd	Gyp. Bd	6	16	Slit	Wide	0.052	92.5	67.0	52	0.826	29.7	39.7	0.75	0.90	31.1	0.95
	2	" "	" "	6	16	Solid	"	0.050	92.5	66.9	47	0.829	34.1	35.3	0.97	1.46	31.1	1.10
	3	LG Fiberbd	(None)	6	-	Slit	Wide	0.052	92.5	67.0	52	0.826	23.9	39.7	0.60	0.64	31.1	0.77
	4	" "	"	6	-	Solid	"	0.050	92.5	66.9	47	0.829	27.2	35.3	0.77	0.92	31.1	0.87
	5	Plywood	Gyp. Bd	30**	30**	Slit	Narrow	0.049	93.0	67.3	49	0.819	30.0	35.5	0.85		31.1	0.96
	6	"	" "	30**	30**	"	"	0.049	93.0	67.3	49	0.819	31.0	35.5	0.87		31.1	1.00
	7	"	" "	30**	30**	"	"	0.049	93.0	67.3	49	0.819	33.0	35.5	0.93		31.1	1.06
	8	Gyp. Bd	Gyp. Bd	12***	8,12***	Slit	Narrow	0.049	93.0	67.3	49	0.819	35.0	35.5	0.99		31.1	1.13
20	9	LG Fiberbd	Gyp. Bd	6	16	Slit	Narrow	0.039	93.0	67.1	46	0.775	18.7	25.8	0.72	0.94	22.3	0.84
	10	" "	" "	6	16	Solid	"	0.040	93.0	67.1	53	0.757	21.3++ ++	29.2	0.73	0.88	22.3	0.96
	11	" "	" "	6	16	"	Wide	0.040	92.5	66.7	53	0.757	26.1	29.2	0.89	1.25	22.3	1.17
	12	LG Fiberbd	(None)	6	-	Slit	Narrow	0.039	93.0	67.1	46	0.775	16.1	25.8	0.62	0.70	22.3	0.72
	13	" "		6	-	Solid	"	0.040	93.0	67.1	53	0.757	18.6	29.2	0.64	0.66	22.3	0.83

(Continued)

Table I (Continued)

* 1/2-Inch-thick low-grade (LG) fiberboard, 1/2-inch-thick gypsum wallboard, or 1/2-inch-thick A-D plywood.

** Adhesive used for these connections only.

*** 8 Inches around the periphery, 12 inches within the interior of the sheet.

\+ Square-ended studs in wide track; in narrow track, ends of flanges of studs were beveled to fit the contour of of the bend fillets of the track.

++ Neglecting the sheathing.

+++ For 18- and 20-gage studs, respectively, steel thicknesses of 0.0496 inch and 0.0376 inch, corresponding to galvanized-sheet thicknesses of 0.0516 inch and 0.0396 inch.

++++ Invalid test; in this test only, failure was confined to local buckling of the stud at the track. In all other tests, failure included buckling away from the track.

Conversion Factors

1 inch = 25.4 mm
1 ksi = 6.89 MPa
1 kip = 4.45 kN

Table II

Lateral-Loading Tests

Gage	Test No.	Sheathing* Exterior Side	Sheathing* Interior Side	Spacing of Screw Fasteners, inches Exterior Side	Spacing of Screw Fasteners, inches Interior Side	Type of Stud	Uncoated Thickness of Stud, inch	Yield Point of Stud Steel, ksi	P_{test} = Maximum Net Lateral Pressure on Specimen, psf	Theoretical Pressure+ Initiating Yielding of Solid Studs with the Measured Thickness and Yield Point: P_{theo}, psf	Theoretical Pressure+ Initiating Yielding of Solid Studs with the Measured Thickness and Yield Point: $\frac{P_{test}}{P_{theo}}$	Theoretical Pressure+ Initiating Yielding of Solid Studs With the Nominal Thickness++ and a Yield Point of 40 ksi: P_{theo}, psf	Theoretical Pressure+ Initiating Yielding of Solid Studs With the Nominal Thickness++ and a Yield Point of 40 ksi: $\frac{P_{test}}{P_{theo}}$
18	14	NG Fiberbd	Gyp. Bd	3, 6**	16	Slit	0.049	42	116.0	103.6	1.12	99.8	1.16
	15	" "	" "	3, 6**	16	Solid	0.049	38	126.4	93.7	1.35	99.8	1.27
	16	NG Fiberbd	None	3, 6**	-	Slit	0.049	42	105.6	103.6	1.02	99.8	1.06
	17	" "	"	3, 6**	-	Solid	0.049	38	108.7	93.7	1.16	99.8	1.09
	18	LG Fiberbd	None	3, 6**	-	Slit	0.049	42	51.7	103.6	0.50	99.8	0.52
	19	" "	"	3, 6**	-	Solid	0.049	38	55.6	93.7	0.59	99.8	0.56
	20	Panel 15	Gyp. Bd	6, 12	16	Slit	0.049	42	135.0	103.6	1.30	99.8	1.35
	21	" "	" "	6, 12	16	Solid	0.049	38	147.0	93.7	1.57	99.8	1.47
	22	Panel 15	Gyp. Bd	15, 30***	30***	Slit	0.049	49	94.4	120.8	0.78	99.8	0.95
	23	" "	" "	15, 30***	15***	"	0.049	49	105.0	120.8	0.87	99.8	1.05
	24	" "	" "	15, 30***	2***	"	0.049	49	104.8	120.8	0.87	99.8	1.05
20	25	NG Fiberbd	Gyp. Bd	6	16	Slit	0.039	46	75.1	91.6	0.82	76.9	0.98
	26	" "	" "	6	16	Solid	0.040	53	93.0	107.7	0.86	76.9	1.21
	27	LG Fiberbd	None	6	-	Slit	0.039	46	50.1	91.6	0.55	76.9	0.65
	28	" "	"	6	-	Solid	0.040	53	51.4	107.7	0.48	76.9	0.67

* 1/2-Inch-thick nail-grade (NG) or low-grade (LG) fiberboard, 1/2-inch-thick gypsum wallboard, or Panel 15, which is 0.3-inch-thick plywood with 10-mil exterior and 2-mil interior aluminum facing sheets.

** Where two numbers are shown, the first is the spacing around the periphery and the second is the spacing within the interior of the sheet.

*** Adhesive used for these connections only.

\+ Neglecting the sheathing; the specimen spans 86 inches c-c roller bearings.

++ For 18- and 20-gage studs, respectively, steel thicknesses of 0.0496 inch and 0.0376 inch, corresponding to galvanized-sheet thicknesses of 0.0516 inch and 0.0396 inch.

Conversion Factors

1 inch = 25.4 mm
1 mil = 0.025 mm
1 ksi = 6.89 MPa
1 psf = 0.048 kPa

Table III

Single-Stud Compression Tests

Nominal Gage	Type of Stud	Uncoated Thickness of Stud, inch	Yield Point of Stud Steel, ksi	Q = AISI Area Factor	Length, inches	Effective Unsupported Length, inches	$\frac{L}{r_{yy}}$ = Maximum Slenderness Ratio for Weak-Axis Buckling	Pe = Euler Weak-Axis Buckling Load Based on Measured Thickness, kips	Ptest = Maximum Total Load on Specimen, kips	Theoretical Load Based on Measured Thickness and Yield Point: Ptheo, kips	Theoretical Load Based on Measured Thickness and Yield Point: Ptest/Ptheo	Theoretical Load Based on Nominal Thickness** and Yield Point: Ptheo, kips	Theoretical Load Based on Nominal Thickness** and Yield Point: Ptest/Ptheo
18	Slit	0.049	49	0.819	20	10*	18	-	11.2	13.78	0.81	11.78	0.95
									10.6		0.77		0.90
									11.7		0.85		0.99
									11.3		0.82		0.96
									11.6		0.84		0.98
									10.8		0.78		0.92
	Solid	0.049	38	0.848	20	10*	18	-	11.0	11.10	0.99	11.78	0.93
									10.6		0.95		0.90
									11.5		1.04		0.98
									10.1		0.91		0.86
									10.2		0.92		0.87
									11.1		1.00		0.94
	Slit	0.052	52	0.826	96	98+	174	3.54	3.15	3.28	0.96	3.16	1.00
									3.47		1.06		1.10
									3.52		1.07		1.11
	Solid	0.049	49	0.819	96	98+	175	3.31	3.62	3.10	1.17	3.16	1.15
									3.45		1.11		1.09
									3.60		1.16		1.14

* For these specimens only, the effective unsupported length is one-half the specimen length, 20 inches, because the ends of each specimen were fixed against rotation during the test.

** For 18-gage studs, steel thickness of 0.0496 inch, corresponding to galvanized-sheet thickness of 0.0516 inch.

\+ Distance between bearing lines of top and bottom half pins.

Conversion Factors

1 inch = 25.4 mm
1 ksi = 6.89 MPa
1 kip = 4.45 kN

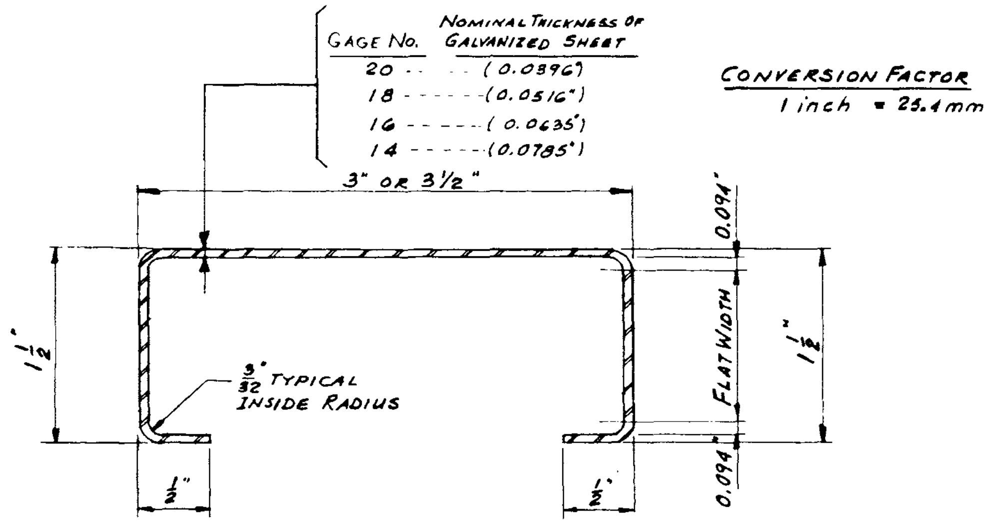

COMMERCIALLY AVAILABLE SUPER-C STEEL STUDS

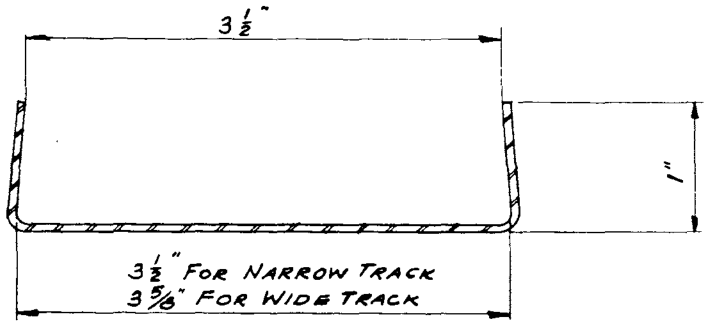

STEEL RUNNER TRACK IN TEST SPECIMEN

SOLID WEB STEEL STUDS

FIGURE 1

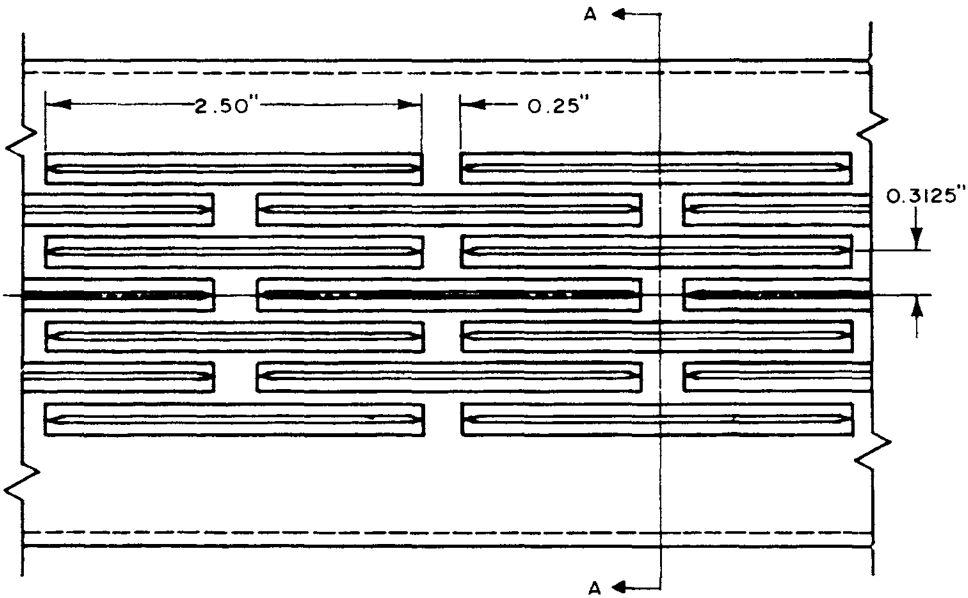

PLAN VIEW OF WEB FACE

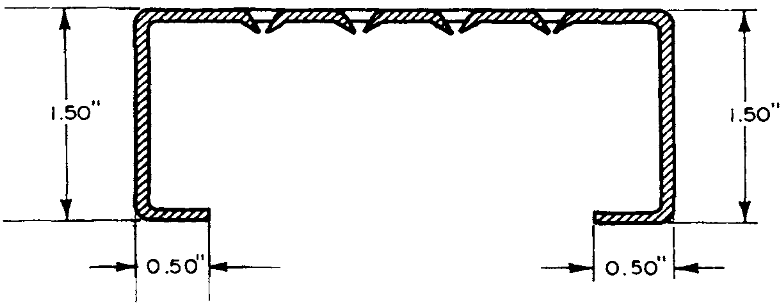

SECTION A-A

1 INCH = 25.4 mm

SLIT WEB STEEL STUDS

FIGURE 2

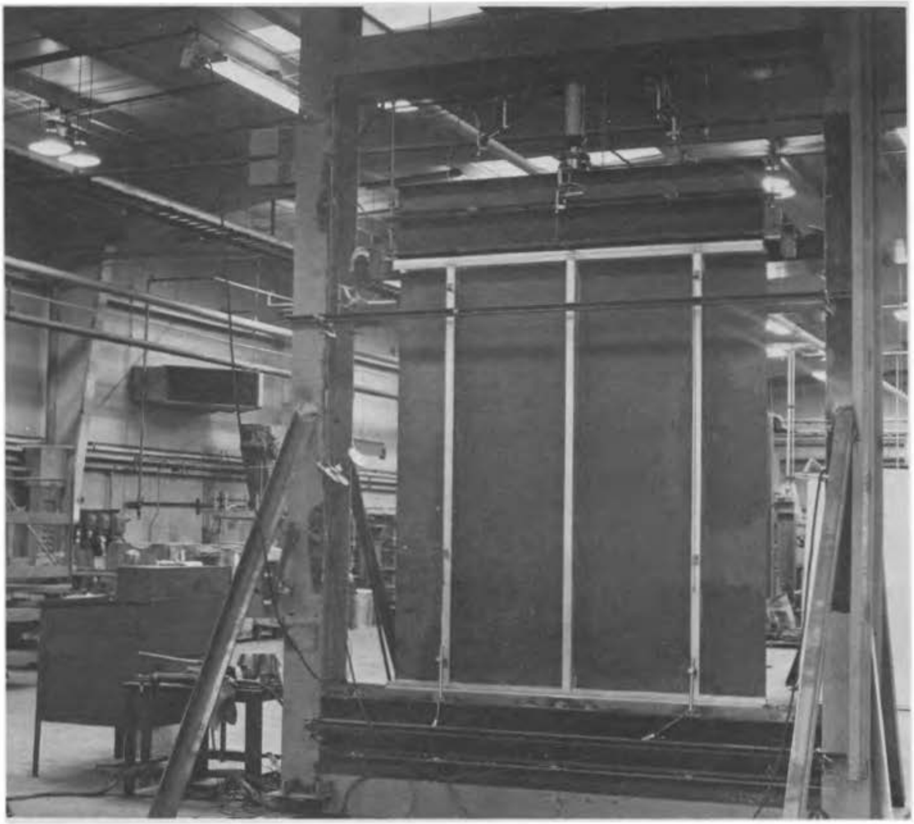

Wall-Compression Test Specimen
With Sheathing on One Side Only

Figure 3.

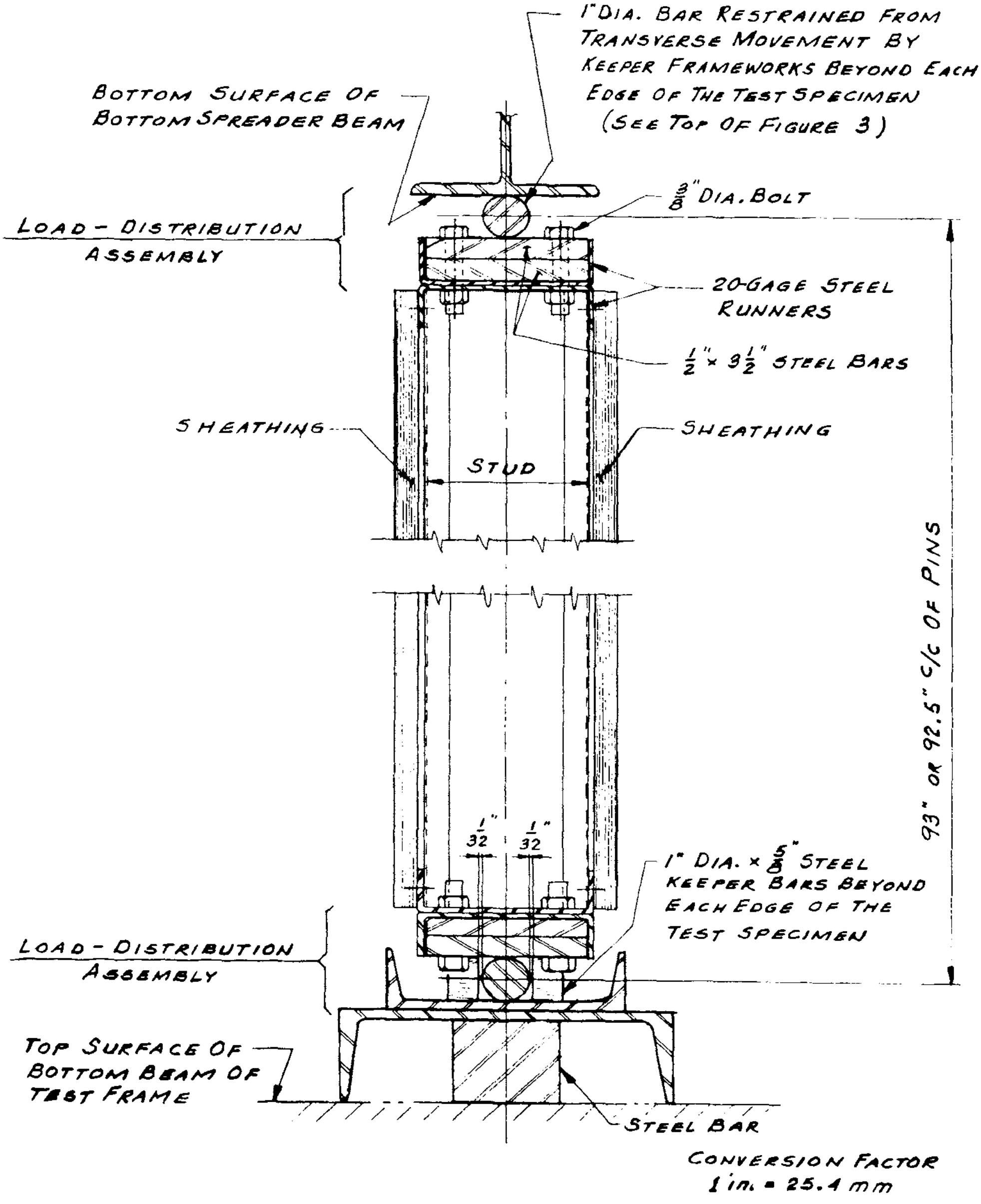

TYPICAL CROSS SECTION THROUGH WALL-COMPRESSION TEST SPECIMEN

FIGURE 4

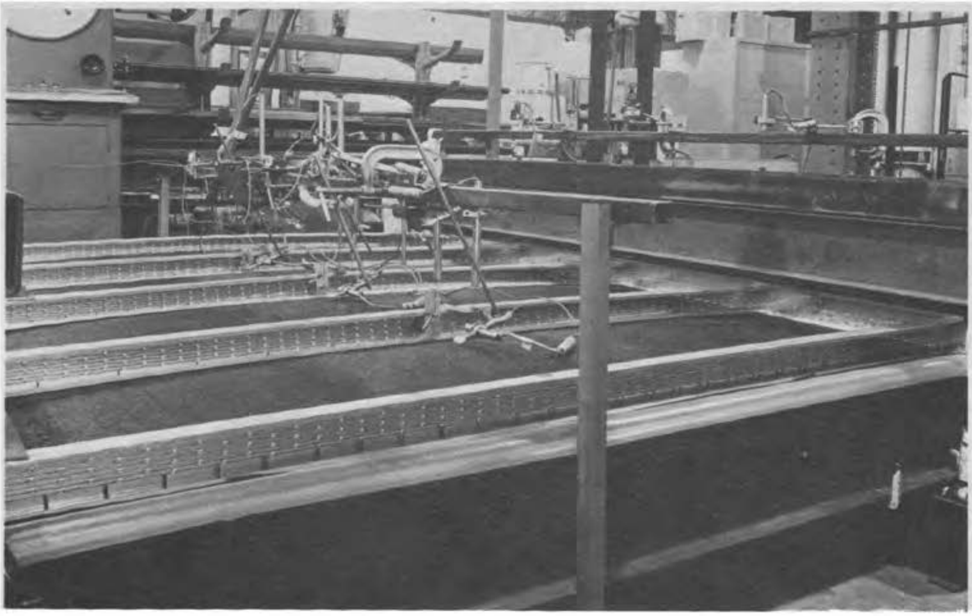

Lateral-Loading Test Specimen
With Sheathing on One Side Only

Figure 5.

Setup for Single-Stud
Compression Tests

Figure 6.

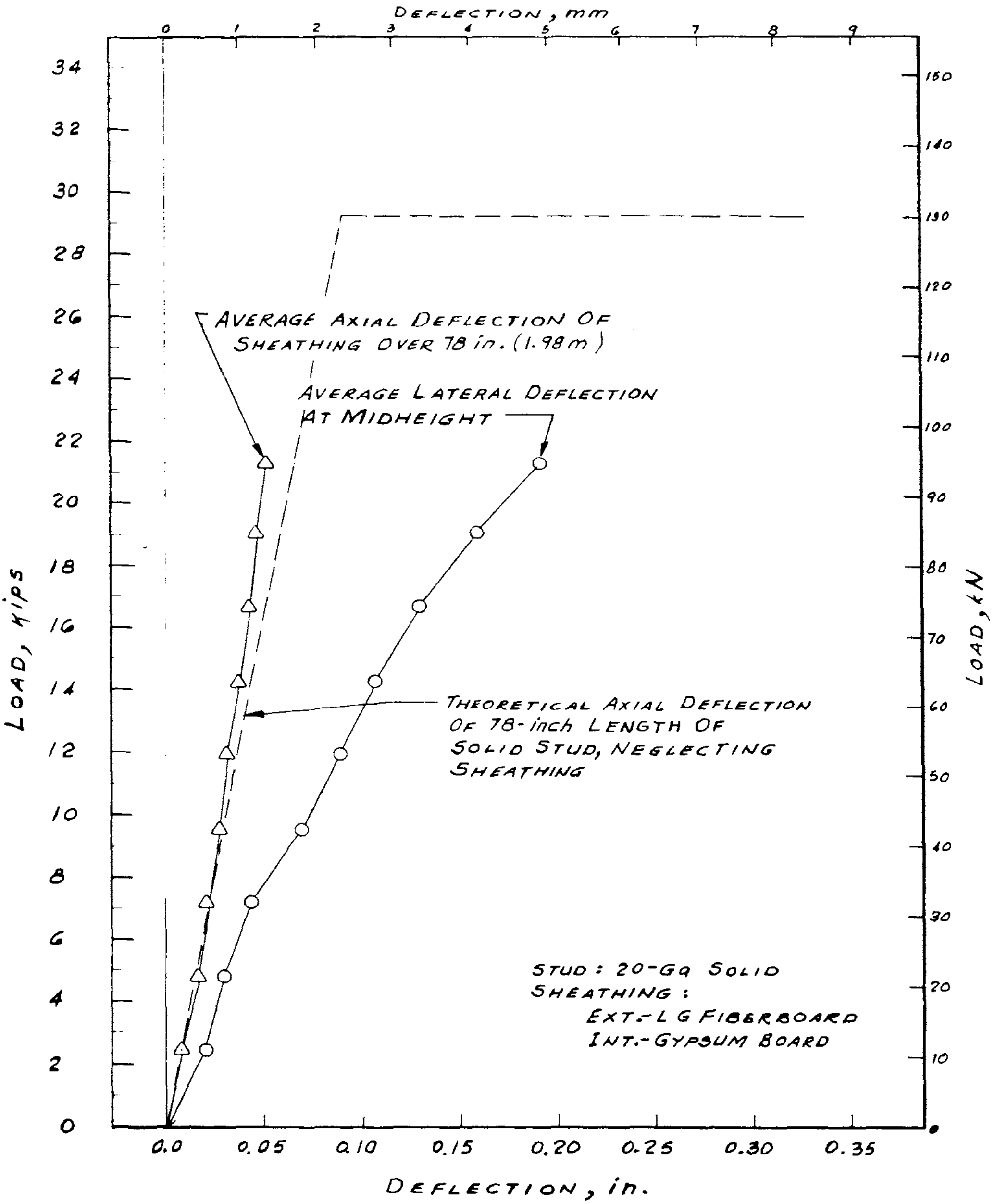

DEFLECTIONS OF WALL-COMPRESSION TEST No. 10

FIGURE 7

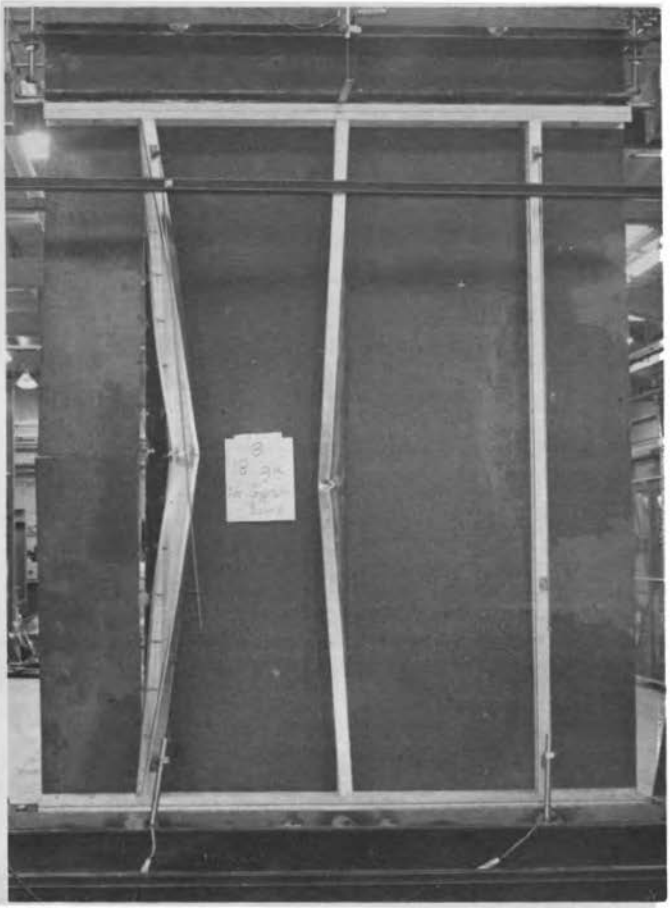

Failure of Wall Compression Test No. 4.

Figure 8.

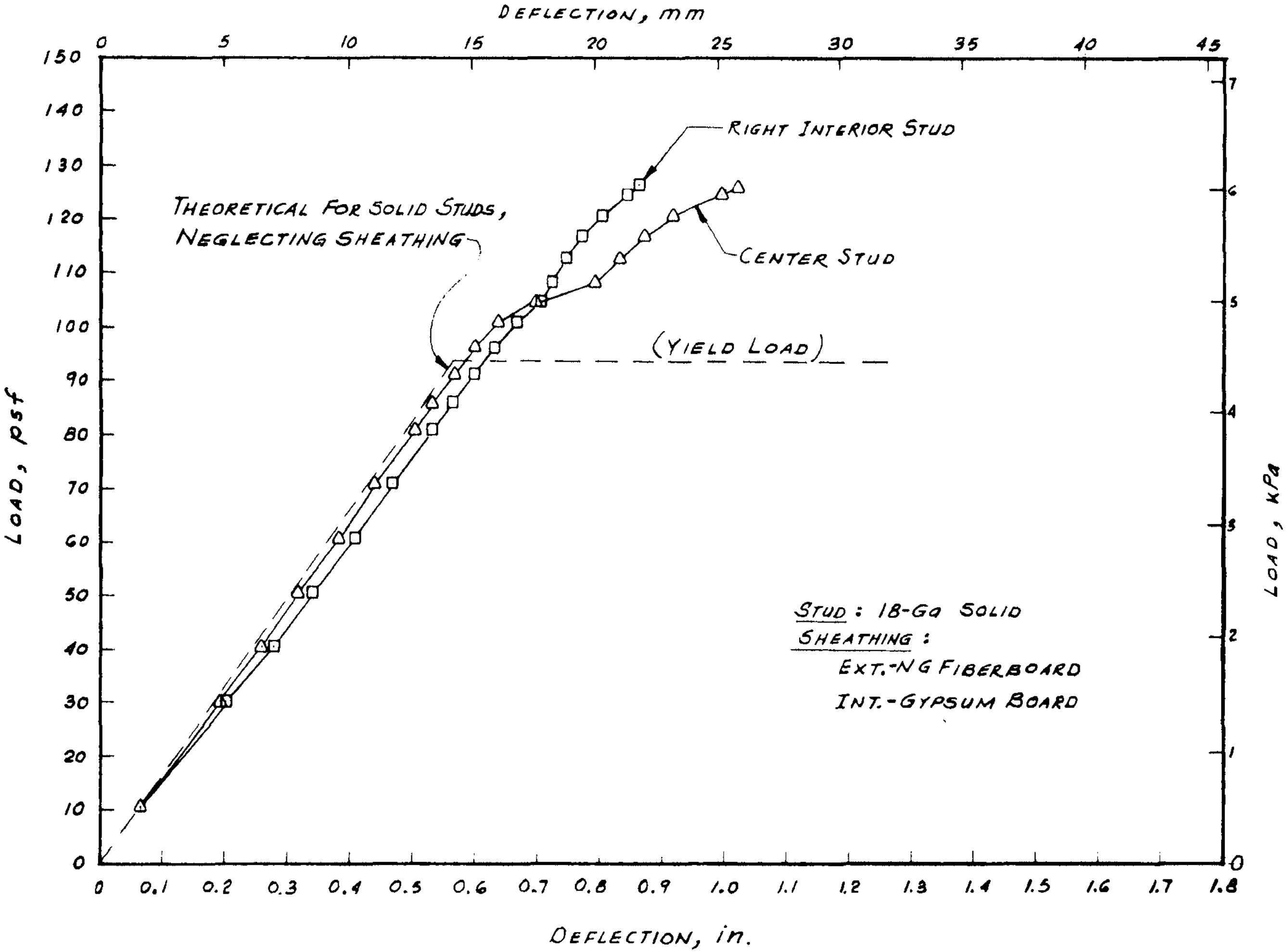

DEFLECTIONS OF LATERAL-LOADING TEST NO. 15

FIGURE 9

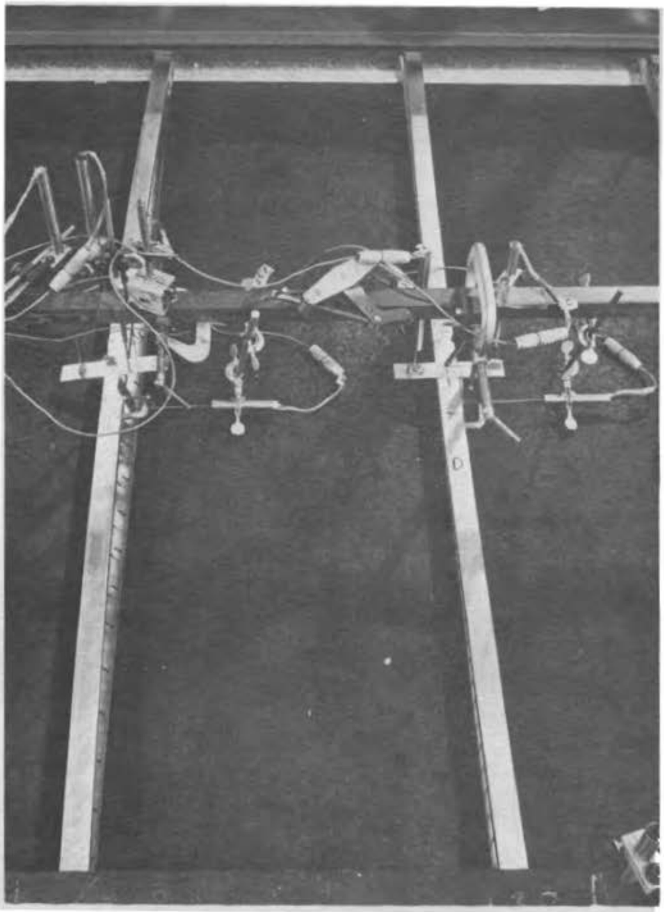

Twisting of Studs in Lateral-Load Test
of Specimen With Sheathing on One Side Only

Figure 10.

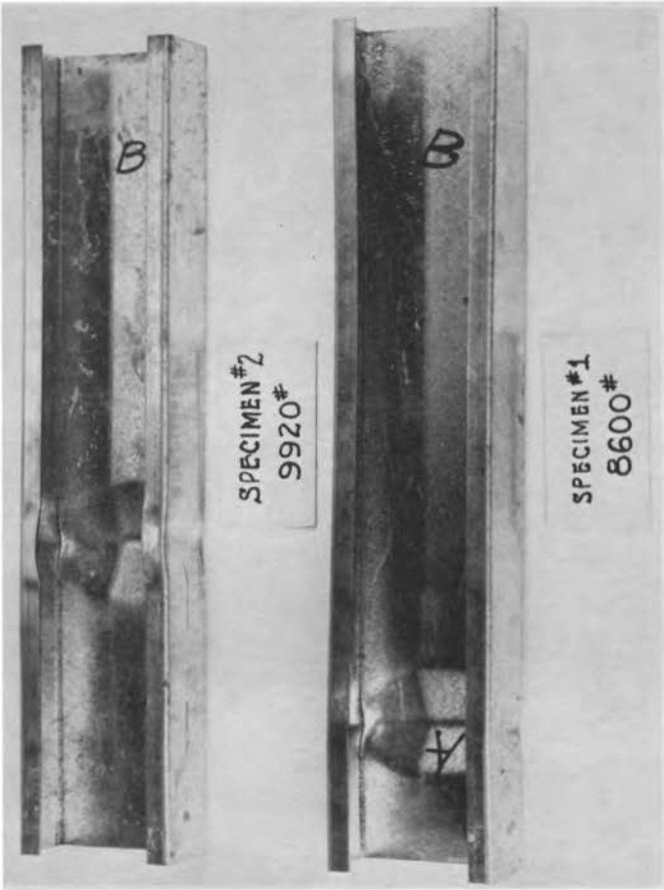

Short Length Local Buckles in
20-Inch-Long (0.51 m) Solid Studs

Figure 11.

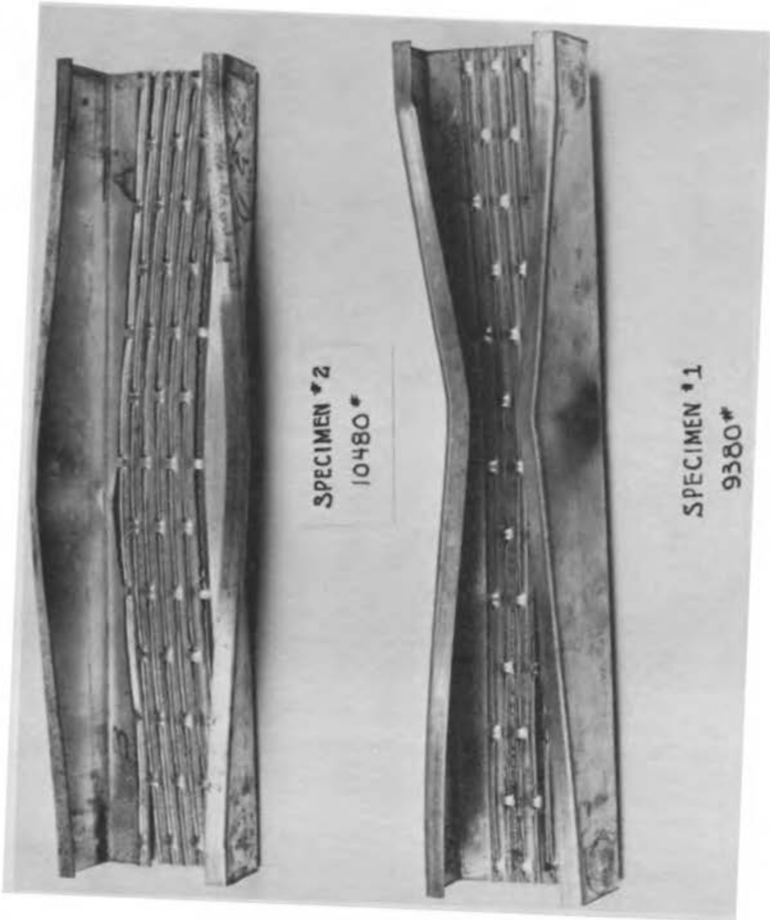

Long-Length Buckles in
20-Inch-Long (0.51 m) Slit Studs

Figure 12.